

Published in final edited form as:

*Nat Struct Mol Biol.* 2013 September ; 20(9): . doi:10.1038/nsmb.2641.

## The N-terminal acetylation of Sir3 stabilizes its binding to the nucleosome core particle

Nadia Arnaudo<sup>1</sup>, Israel S. Fernández<sup>1</sup>, Stephen H. McLaughlin<sup>1</sup>, Sew Y. Peak-Chew<sup>1</sup>, Daniela Rhodes<sup>1,2</sup>, and Fabrizio Martino<sup>1</sup>

<sup>1</sup>Structural Studies Division, Medical Research Council - Laboratory of Molecular Biology, Cambridge, UK

### Abstract

The N-terminal acetylation of Sir3 is essential for heterochromatin establishment and maintenance in yeast, but its mechanism of action is unknown. The crystal structure of the N-terminal acetylated BAH domain of *S.cerevisiae* Sir3 bound to the nucleosome core particle revealed that the N-terminal acetylation stabilizes the interaction of Sir3 with the nucleosome. Additionally, we present a new method for the production of protein-nucleosome complexes for structural analysis.

SIR (Silent Information Regulator) proteins belong to a family of chromatin regulatory factors, such as Heterochromatin Protein 1 and Polycomb, that are thought to function by folding the chromatin fiber into a highly compacted, transcriptionally silent, structure called heterochromatin<sup>1</sup>. Heterochromatin plays a crucial role in chromosome segregation, stabilization of repeated DNA sequences and cell type determination. Despite of their functional importance, it is not understood at the structural level how heterochromatic proteins recognize the NCP (Nucleosome Core Particle), the basic unit of chromatin, and how they fold the chromatin fiber into high order structures that induce transcriptional gene silencing. In budding yeast, heterochromatin is present at the mating type loci and subtelomeric regions where it is established and maintained by the SIR complex, formed by Sir2, Sir3 and Sir4. Sir3 plays a crucial role in binding the NCP through its N-terminal BAH (Bromo Adjacent Homology) domain and possibly its C-terminal AAA+ (ATPases Associated with diverse cellular Activities) domain<sup>2-5</sup>. Importantly, Sir3 is acetylated on its N-terminus and lack of this modification impairs the spreading of Sir3, and thus of silencing, along the chromatin fiber<sup>6-9</sup>. The molecular mechanism behind the function of Sir3 N-terminal acetylation is unknown. Previous crystal structures of the BAH domain in complex with the NCP could not answer this question because they contained unacetylated BAH<sup>10,11</sup>. On a more general note, because more than 80% of eukaryotic proteins are N-terminally acetylated it is important to understand how this post-translational modification affects protein structure and function<sup>12</sup>.

Correspondence should be addressed to F.M.: [fabrizio@mrc-lmb.cam.ac.uk](mailto:fabrizio@mrc-lmb.cam.ac.uk).

<sup>2</sup>Present address: School of Biological Sciences, Nanyang Technological University, Singapore (R.D.).

#### Author Contributions

D.R., F.M. And N.A. Designed the experiments. F.M. And N.A. purified all the proteins, DNA and complexes used, prepared, optimized and cryo-protected the crystals, solved the structure and wrote the manuscript. I.S. froze the crystals. F.M., N.A., I.S. collected the X-ray diffraction data. N.A. and S.H.M performed the binding experiments. S.Y.P.-C. performed the MALDI. D.R. revised the manuscript.

#### Accession code:

Coordinates and structure factors have been deposited in the Protein Data Bank under accession code 4LD9.

#### Competing financial interests

The authors declare no competing financial interests.

To investigate whether the N-terminal acetylation of Sir3 regulates its binding to the NCP we expressed a long version of the BAH spanning Sir3 first 380 amino acids. This is the N-terminal fragment of Sir3 that best complements the silencing defect of a *sir3* strain<sup>13</sup>. We expressed the BAH both in insect cells where Met1 is removed and the Ala2 N-terminus acetylated and in bacteria where Met1 is cleaved but Ala2 is not acetylated. MALDI analysis and SDS-PAGE confirmed that the two proteins are indistinguishable except for the N-terminal acetylation present only in the protein expressed in insect cells (Supplementary Fig. 1a-c). Quantitative EMSAs (Electro Mobility Shift Assay) revealed that the N-terminal acetylation increases the affinity of the BAH for the NCP by at least a factor of two (Fig. 1a,b). To understand how the N-terminal acetylation affects the chromatin binding properties of Sir3, we determined the crystal structure of the N-terminally acetylated BAH bound to the NCP. Since conventional matrix-based purification methods often cause sample heterogeneity and losses, we developed a new matrix-free method. In this method, the BAH-NCP complexes were precipitated with PEG and re-suspended in a buffer at a concentration suitable for crystallization trials with a final recovery of 90% of the initial complex. The purified complexes were highly homogeneous as revealed by the presence of only one well-defined band in native gels (Supplementary Fig. 2a, lane 3). Importantly, we isolated only BAH-NCP complexes and not free components, since no free NCPs or free BAH precipitate at the PEG concentration used (Supplementary Fig. 2a, lane 4 and Supplementary Fig. 2b, lane 2). We analyzed the subunit composition of the purified BAH-NCP complex against known amounts of the NCP and the BAH. From this analysis we estimated that the complex has a stoichiometry of two molecules of BAH per NCP (Supplementary Fig. 2c,d).

The structure of the N-terminal acetylated BAH in complex with the NCP was solved at 3.3Å resolution and it was superimposed to the structure of the unacetylated BAH bound to NCP (Fig. 2a,b). In addition to the multiple interactions involved in the recognition of the NCP by the BAH reported previously<sup>10</sup>, we observe a set of additional interactions arising from the acetylated N-terminus of Sir3 (Fig. 2c-e). As a result, loop3 and helix8 of Sir3 BAH are positioned closer to the histone core surface (Fig. 2b,c,e). In particular, the side chain of Asn80, located in loop3, is within hydrogen-bonding distance to the side chains of H2B Arg93 and H4 Glu74 (Fig. 2c and Supplementary Fig. 3b,c). Asn80 is part of a tight network of interactions where the position of H2B Arg93 side chain is stabilized by H4 His75, whereas H4 Glu74 side chain is held in place by a potential hydrogen bond with H4 Arg67 (Fig. 2c and Supplementary Fig. 3d). Loop3 forms a pocket-like structure that holds H3 Lys79 in place like a key in a lock (Fig. 2c). The presence of several acidic amino acids in loop3 suggests that the side chain of H3 Lys79 can assume different orientations in the pocket, providing an explanation for the poor electron density observed for H3 Lys79. Well-defined experimental densities could be assigned to the other residues forming the pocket (Supplementary Fig. 3b-d).

Importantly, the acetylated N-terminus interacts with loop3 and stabilizes its interactions with the core histones. In particular, Ala2 interacts with Val82 and Val83 and pushes loop3 against the histone core (Fig. 2c). The position of Ala2 is determined by the interaction of the N-terminal acetyl group with the main chain amine of Leu143 and the aromatic ring of Trp142 (Fig. 2d and Supplementary Fig. 3a). The aromatic ring of Trp142 is rotated toward the methyl moiety of the acetyl group that is a different conformation compared to the unacetylated BAH (Fig. 2d).

The interaction between the N-terminal acetyl group and loop3 appears to generate a rotation of the whole BAH toward the surface of the NCP. As a consequence, helix8 is positioned closer to the core histones compared to its position in the unacetylated BAH (Fig. 2a,b). Helix8 was crucial for silencing and it has been proposed to bind nucleosomal DNA<sup>2</sup>.

In our structure, helix8 was not facing DNA, but histones H3 and H4 (Fig. 2a,b,e). In particular, BAH Lys202 was within hydrogen bonding distance to H4 Glu63, while BAH Lys209 likely interacts with H4 Asp24 and H3 Glu73 (Fig. 2e). Importantly, these interactions were not described for the previous unacetylated BAH-NCP structure because helix8 was located too far from the histone core surface (Fig. 2e).

The new N-terminal acetylation-dependent interactions between the BAH and the NCP we observe correlate very well with *in vivo* data. Indeed, Lys209Asn and Lys202Glu in helix8 have been identified as dominant negative mutations<sup>2</sup>. Moreover, mutations of BAH Asn80, of H3 Lys79 and of the amino acids around H3 Lys79 cause severe silencing defects<sup>8,14</sup>. Furthermore, H3 Lys79 is methylated in transcribed regions and there is evidence that methylated H3 Lys79 prevents Sir3 mis-localization *in vivo* and also reduces Sir3 binding *in vitro*<sup>9,15</sup>. Our structure suggests that methylation of H3K79 would create repulsion with the residues in the BAH loop3 leading to the disruption of the BAH-NCP complex.

Our structure provides an interpretation for the effects of mutations at BAH Ala2 that affect Sir3 function. It is important to note that, in all previous structures containing the unacetylated BAH, the N-terminus of Sir3 (from Ala2 to Gly10) was disordered<sup>10,11,13</sup>. Instead, in our acetylated BAH-NCP complex, we observe a short helix (Asp9 to Thr4) that probably is necessary to ensure that the acetylated N-terminus is in the correct position to interact with Sir3 loop3 (Fig. 2d and Supplementary Fig. 3a). The short N-terminal helix is an important structural component of the N-terminus because mutations in this helix cause a silencing phenotype<sup>8</sup>. Yeast strains carrying the Ala2Gln mutation exhibit a strong silencing defect at telomeres and *HML* consistent with the loss of Sir3 spreading<sup>6,7</sup>. Ala2Gln would be displaced because it is unacetylated and the side chain of the unprocessed Met1 would clash with Trp142. Finally the long side chain of Gln would clash with the short N-terminal helix (Fig. 2d). Similarly, amino acids with a long side chain placed in position 2 would clash against the BAH N-terminal helix. Consistent with this interpretation, Ala2 mutations to Lys, Glu, Asp present strong phenotypes<sup>6</sup>.

In summary, our work provides a biochemical and structural explanation for the importance of Sir3 N-terminal acetylation in NCP recognition and in the establishment of gene silencing. We propose that the N-terminal acetylation stabilizes the interaction between Sir3 and the NCP by positioning loop3 and helix8 within hydrogen-bonding distance to the histone core surface. This proposal is substantiated by the excellent correlation between genetic and structural data and hence the biological relevance of the interactions described. On a more general note, our structure suggests that the common N-terminal acetylation of proteins plays an important role in the stabilization of protein-protein interactions.

## Online Methods

### Preparation and crystallization of BAH-NCP complexes

Sir3 BAH domain (1-380 or 1-229) was cloned in pOPIN-E vector (Oxford Protein Expression Facility) with a C-terminus hexa-His tag. The proteins were expressed in *BL21(DE3) pLysS E. coli* 20°C over night or in Sf21 insect cell line for three days after infection. Sir3 BAH was purified by chromatography on Ni-NTA (Qiagen) followed by heparin, S/Q and Superdex S200 19/60 (GE Healthcare). The proteins were concentrated to 30 mg/ml in 300 mM NaCl, 50 mM TRIS pH 8, 1 mM EDTA, 1 mM TCEP and flash frozen in liquid nitrogen. Recombinant *Xenopus* core histone were expressed, purified and reconstituted with the Widom 601 DNA sequence into NCP following K. Luger's protocol<sup>16</sup>. The complex between the N-terminally Ac-Sir3 BAH domain and cy5-labeled NCP was assembled by mixing the BAH domain with NCPs at 2  $\mu$ M in a 2:1 BAH:NCP molar ratio. The complex was then purified by differential precipitation with PEG 6000

(Hampton). BAH-NCP crystals were obtained from BAH fragments of different length, but only one, from amino acid 2 to 229, produced crystals that diffracted at resolution higher than 4Å. Crystals of the complex were grown by vapor diffusion at 20°C in MRC-MAXI plates by mixing 0.5 µl of the complex (at 12µM) with 0.5 µl of 50 mM MES pH 6.5, 12% PEG 400, 12 mM MnCl<sub>2</sub>, 100 mM NaCl, 10 mM EDTA. After six weeks, crystals were soaked gradually in increasing concentration of PEG 400 (up to 27%). The soaked crystals were then flash frozen in liquid nitrogen for data collection.

### Purification of BAH-NCP complexes by differential PEG precipitation

The BAH-NCP complexes were incubated with 5% PEG 6000 for 5 minutes and centrifugation was carried out at 10000g for 10 minutes. The pellet was resuspended in 20 mM TEA pH 7.4, 200 mM NaCl, 1 mM EDTA, 1 mM TCEP, at a final concentration of 12 µM, and analyzed on both native polyacrylamide gel electrophoresis (PAGE) and SDS-PAGE gels to assess, respectively, the purity and the composition of the sample.

### MALDI-MS analyses

Sir3 BAH expressed in Baculovirus and *E. coli* were dialyzed in 20mM ammonium bicarbonate. 1µl of proteins followed by 1 µl of 2,5-DHB (2,5-Dihydroxybenzoic acid, saturated solution in 10% acetonitrile/0.1% trifluoroacetic acid) matrix solution were deposited and mixed on the MALDI target. All MALDI-MS experiments were carried out on an Ultraflex III TOF/TOF mass spectrometer (Bruker Daltonics, Bremen, Germany). ISD (In-Source Decay) analyses were acquired in positive reflectron mode. ISD spectra were externally calibrated with standard peptides mixture consisted of [M+H]<sup>+</sup> 904.4861, 1296.6848, 1645.8962, 2093.0862, 2932.5879 and 3657.9294. FlexAnalysis 3.0 and Biotoools 3.2 (Bruker Daltonics) were used for analysis and fragments assignment. Fragments were assigned with mass accuracies of <0.5Da. The MALDI-MS experiment confirmed the presence of the N-terminal acetylation only in Sir3 BAH expressed with the Baculovirus system. Indeed, in Sir3 BAH expressed in bacteria the Met1 was removed but Ala2 was not acetylated.

### Electrophoretic mobility shift assays

Cy5-labeled NCPs (0.2 µM) were incubated with increasing concentrations of unacetylated (expressed in *E. coli*) or acetylated (expressed in Baculovirus) Sir3 BAH domain in 10 mM TEA pH 7.4, 1 mM EDTA, 50 mM NaCl, 1 mM TCEP. Samples were then analyzed on a 5% native PAGE run in 0.2× TB buffer and the fluorescence was detected with the Typhoon system (GE Healthcare Life Sciences).

The affinity was determined by measuring the disappearance of the band corresponding to the NCP substrate. The binding analysis was repeated in triplicate and the measurements plotted with the corresponding errors. The binding curve shows that 50% of substrate saturation is reached at 0.4 µM of acetylated BAH compared to 0.8 µM of unacetylated BAH.

### X-ray data collection, processing, model building and refinement

X-ray diffraction data were collected at I24 beamline equipped with a Pilatus3-6M detector, at the Diamond Light Source, Didcot, UK, and processed using XDS<sup>17</sup>.

The structure was solved by molecular replacement using PHASER from the CCP4i suite<sup>18</sup> and a search model containing two rigid bodies: Sir3 BAH (2FL7) deleted for the N-terminus (aa 1-11) and loop3 (aa 75-83) and the NCP containing the Widom 601 DNA sequence (3LZ0). The model was refined with Phenix<sup>19</sup> and additional model building was done with Coot. In parallel, the dataset was refined with Refmac5, with restraints on alpha

helices and DNA base-pairing from the PROSMART and LIBG tools<sup>20</sup>. Both Phenix and Refmac5 gave a similar solution with equivalent statistics. All molecular graphics were prepared using PyMOL.

## Supplementary Material

Refer to Web version on PubMed Central for supplementary material.

## Acknowledgments

We thank G. Murshudov, F. Long, R. Nicholls, P. Emsley and H. Powell for trouble shooting and sharing tools with the softwares: Refmac5, LibG, Prosmart, Coot and iMosflm. We thank M. Lamers and the K. Nagai's laboratory for critical discussion of the results. We thank M. Yu for helping with the usage of the I24 beamlines at DLS (Diamond Light Source).

F.M. is supported by Swiss National Fund (PBGEP3-123695), European Molecular Biology Organization Long Term Fellowship (ALTF419-2009) and Marie Curie Intra European Long Term Fellowship (FP7-PEOPLE-2009-IEF-251794). N.A. is supported by the EU FP7 Marie Curie Initial training Nucleosome 4D network (4609511-238176). The project was supported by the Medical Research Council (MC-A025-5PJ80).

## References

- Buhler M, Gasser SM. Silent chromatin at the middle and ends: lessons from yeasts. *EMBO J.* 2009; 28:2149–61. [PubMed: 19629038]
- Buchberger JR, et al. Sir3-nucleosome interactions in spreading of silent chromatin in *Saccharomyces cerevisiae*. *Mol Cell Biol.* 2008; 28:6903–18. [PubMed: 18794362]
- Cubizolles F, Martino F, Perrod S, Gasser SM. A homotrimer-heterotrimer switch in Sir2 structure differentiates rDNA and telomeric silencing. *Mol Cell.* 2006; 21:825–36. [PubMed: 16543151]
- Ehrentraut S, et al. Structural basis for the role of the Sir3 AAA+ domain in silencing: interaction with Sir4 and unmethylated histone H3K79. *Genes Dev.* 2011; 25:1835–46. [PubMed: 21896656]
- Onishi M, Liou GG, Buchberger JR, Walz T, Moazed D. Role of the conserved Sir3-BAH domain in nucleosome binding and silent chromatin assembly. *Mol Cell.* 2007; 28:1015–28. [PubMed: 18158899]
- Wang X, Connelly JJ, Wang CL, Sternglanz R. Importance of the Sir3 N terminus and its acetylation for yeast transcriptional silencing. *Genetics.* 2004; 168:547–51. [PubMed: 15454564]
- Ruault M, De Meyer A, Loidice I, Taddei A. Clustering heterochromatin: Sir3 promotes telomere clustering independently of silencing in yeast. *J Cell Biol.* 2011; 192:417–31. [PubMed: 21300849]
- Sampath V, et al. Mutational analysis of the Sir3 BAH domain reveals multiple points of interaction with nucleosomes. *Mol Cell Biol.* 2009; 29:2532–45. [PubMed: 19273586]
- van Welsem T, et al. Synthetic lethal screens identify gene silencing processes in yeast and implicate the acetylated amino terminus of Sir3 in recognition of the nucleosome core. *Mol Cell Biol.* 2008; 28:3861–72. [PubMed: 18391024]
- Armache KJ, Garlick JD, Canzio D, Narlikar GJ, Kingston RE. Structural basis of silencing: Sir3 BAH domain in complex with a nucleosome at 3.0 Å resolution. *Science.* 2011; 334:977–82. [PubMed: 22096199]
- Wang F, et al. Heterochromatin protein Sir3 induces contacts between the amino terminus of histone H4 and nucleosomal DNA. *Proc Natl Acad Sci U S A.* 2013; 110:8495–500. [PubMed: 23650358]
- Arnesen T. Towards a functional understanding of protein N-terminal acetylation. *PLoS Biol.* 2011; 9:e1001074. [PubMed: 21655309]
- Connelly JJ, et al. Structure and function of the *Saccharomyces cerevisiae* Sir3 BAH domain. *Mol Cell Biol.* 2006; 26:3256–65. [PubMed: 16581798]
- Park JH, Cosgrove MS, Youngman E, Wolberger C, Boeke JD. A core nucleosome surface crucial for transcriptional silencing. *Nat Genet.* 2002; 32:273–9. [PubMed: 12244315]

15. Martino F, et al. Reconstitution of yeast silent chromatin: multiple contact sites and O- AADPR binding load SIR complexes onto nucleosomes in vitro. *Mol Cell*. 2009; 33:323–34. [PubMed: 19217406]
16. Luger K, Mader AW, Richmond RK, Sargent DF, Richmond TJ. Crystal structure of the nucleosome core particle at 2.8 Å resolution. *Nature*. 1997; 389:251–60. [PubMed: 9305837]
17. Kabsch W. Integration, scaling, space-group assignment and post-refinement. *Acta Crystallogr D Biol Crystallogr*. 2010; 66:133–44. [PubMed: 20124693]
18. Winn MD, et al. Overview of the CCP4 suite and current developments. *Acta Crystallogr D Biol Crystallogr*. 2011; 67:235–42. [PubMed: 21460441]
19. Afonine PV, et al. Towards automated crystallographic structure refinement with phenix.refine. *Acta Crystallogr D Biol Crystallogr*. 2012; 68:352–67. [PubMed: 22505256]
20. Nicholls RA, Long F, Murshudov GN. Low-resolution refinement tools in REFMAC5. *Acta Crystallogr D Biol Crystallogr*. 2012; 68:404–17. [PubMed: 22505260]

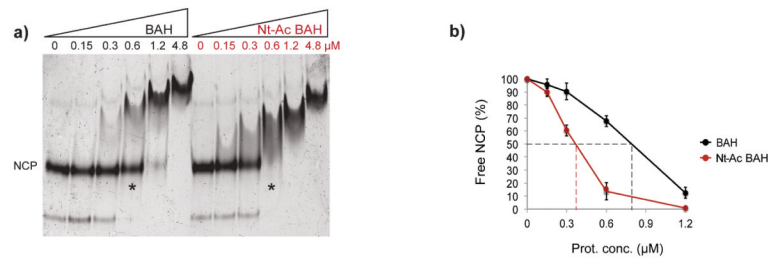


**Figure 1.**

Sir3 N-terminal acetylation increases Sir3 BAH affinity for NCPs

(a) Native-PAGE of fluorescently-labeled NCPs incubated with increasing concentrations of unacetylated (black, BAH) or acetylated (red, Nt-Ac BAH) BAH. Asterisks indicate the titration point with the largest difference in substrate saturation between the acetylated and unacetylated BAH. (b) Quantification of Sir3 BAH binding to NCPs from panel a. The mean value ( $\pm$  standard deviation) of the percentage of unbound NCPs from three independent experiments is plotted against the BAH concentration. The concentration of BAH required for 50% binding to the NCP is indicated by a dashed line

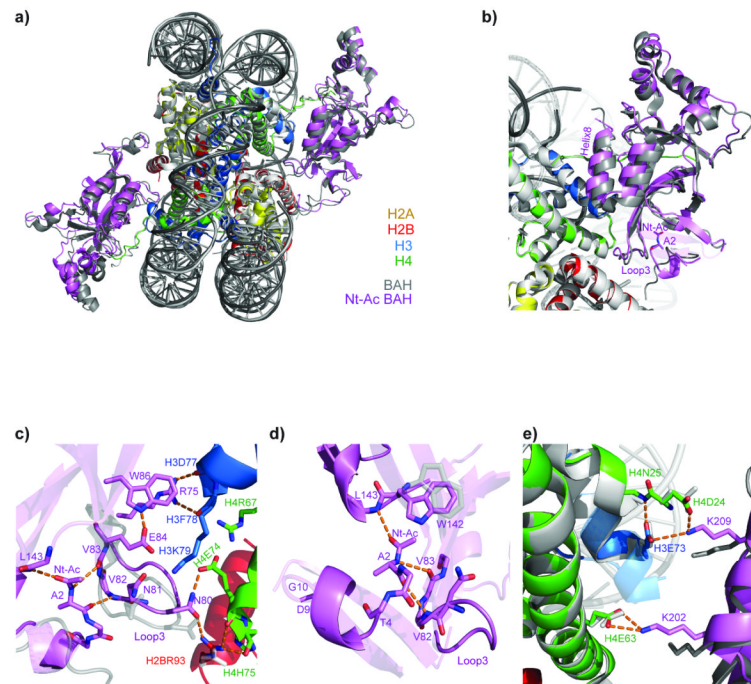


**Figure 2.**

Sir3 N-terminal acetylation stabilizes the interaction of Sir3 BAH with the NCP

(a) Superposition of the structures of the N-terminally acetylated (pink) and unacetylated (grey)<sup>10</sup> BAH in complex with the NCP. (b) Detailed view of Ala2 (A2), N-ter-acetyl group (Nt-Ac), Loop3 and Helix8. (c) Detailed view of the interactions between the acetylated N-terminus of Sir3 and Loop3. (e) Close-up view of Sir3 Helix8–histone core interactions. (d) Detailed view of the acetylated Sir3 N-terminus.